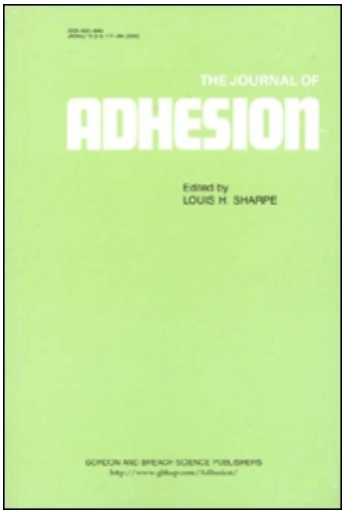

The Journal of Adhesion
Publication details, including instructions for authors and subscription information:
http://www.informaworld.com/smpp/title~content=t713453635

Modelling the Fracture Behaviour of Adhesive Joints

A. J. Kinloch[a]; C. C. Lau[a]; J. G. Williams[a]
[a] Department of Mechanical Engineering, Imperial College of Science, Technology and Medicine, London, UK

To cite this Article Kinloch, A. J. , Lau, C. C. and Williams, J. G.(1996) 'Modelling the Fracture Behaviour of Adhesive Joints', The Journal of Adhesion, 59: 1, 217 — 224
To link to this Article: DOI: 10.1080/00218469608011090
URL: http://dx.doi.org/10.1080/00218469608011090

J. Adhesion, 1996, Vol. 59, pp. 217–224
Reprints available directly from the publisher
Photocopying permitted by license only

Modelling the Fracture Behaviour of Adhesive Joints*

A. J. KINLOCH, C. C. LAU and J. G. WILLIAMS

Department of Mechanical Engineering, Imperial College of Science, Technology and Medicine, Exhibition Rd., London, SW7 2BX, UK

(In final form February 6, 1996)

The present work has defined an adhesive fracture energy, G_a, for the peel testing of flexible laminates. The values of G_a characterises the fracture of the laminate and is considered to be a "geometry-independent" parameter which reflects (i) the energy to break the interfacial bonding forces and (ii) the energy dissipated *locally* ahead of the peel front in the plastic or viscoelastic zone. We have shown that in order to determine this true adhesive fracture energy, G_a, that the following energy terms must be considered: (i) the stored strain-energy in the peeling arm, (ii) the energy dissipated during tensile deformation of the peeling arm, and (iii) the energy dissipated due to bending of the peeling arm. The analysis proposed yields quantitative expressions for these various energy dissipation terms and, in particular, considers the energy dissipated due to bending of the peeling arm. Another important feature of the analysis is the modelling of the region below the peel front as an elastic beam on an elastic foundation, such that the peeling arm does not act as a truly built-in beam and root rotation at the peel front is allowed. The analysis described in the present paper has been employed for four different laminates. The values of the local angle, θ_0, at the peel front from the theoretical calculations have been shown to be in excellent agreement with the experimentally measured values, a small-scale peel test rig having been built so that the peel test, as a function of applied peel angle, θ, thickness, h, of peeling arm and rate of test, could be observed and photographed using a stereo-optical microscope. The value of the adhesive fracture energy, G_a, (*i.e.* the "fully corrected" value) for each laminate is indeed shown to be a "material parameter".

KEY WORDS: Fracture mechanics; adhesive fracture energy; flexible laminate; packaging; peel tests; peel angle; peeling energy; polyethylene; aluminum foil; PET.

1. INTRODUCTION

The peel test is illustrated schematically in Figure 1 and is one of the most frequently used test methods for assessing the failure of flexible laminates, such as those employed in the packaging and electronic industries. It has, therefore, been extensively studied[1–8] and a large amount of experimental and theoretical work exists on the effects of such parameters as the peel angle employed, the thickness of the mateirals, the degree of intrinsic adhesion acting between the materials, the effects of test rate and temperature, etc. The present work examines the peeling of flexible

*Presented at the International Adhesion Symposium, *IAS'94 Japan*, at the 30th Anniversary Meeting of the Adhesion Society of Japan, Yokohama, Japan, November 6–10, 1994.

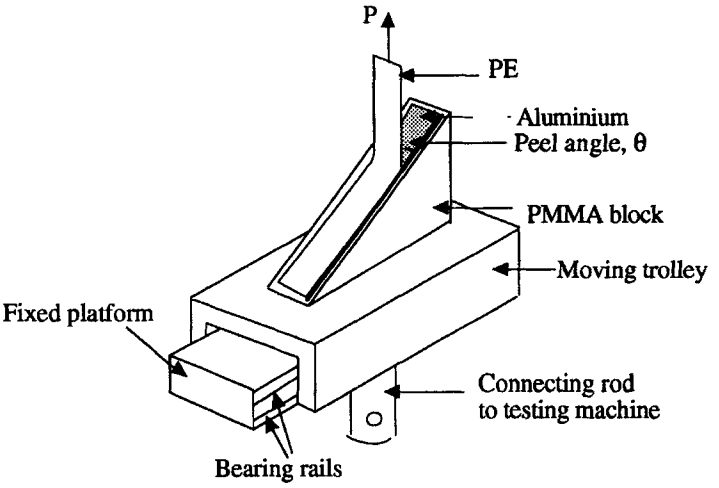

FIGURE 1 The peel test rig for constant peel angle tests.

laminates and, in particular, considers the effects of plastic bending of the peeling arm. A major aim is to derive quantitative expressions for the energy dissipated by plastic deformation due to bending of the beam and thereby to correct the measured peel force for such energy losses. An novel aspect in solving this problem is to model the peel test as an elastic beam on an elastic foundation and to consider the role of root rotation of the peel front. Thus, it is hoped that a true adhesive fracture energy, G_a, may be obtained which is independent of the geometry of the peel test. The validity of this modelling will be examined by conducting peel tests on the stage of a stereo-optical microscope so that the local angle, θ_0, at the peel front can be experimentally measured and compared with the theoretically calculated values. Also, in order to validate the analysis proposed, the independence of the calculated values of G_a for a given laminate from such factors as the applied peel angle, θ, and thickness, h, of the peeling arm will also be explored.

2. THEORETICAL

2.1. Basic Concepts

The adhesive fracture engery, G_a, may be derived from an energy-balance argument, such that:

$$G_a = \frac{1}{b}\left(\frac{dU_{ext}}{da} - \frac{dU_s}{da} - \frac{dU_{dt}}{da} - \frac{dU_{db}}{da}\right) \tag{1}$$

where:

dU_{ext} is the external work
dU_s is the stored strain energy in the peeling arm

dU_{dt} is the energy dissipated during tensile deformation of the peeling arm
dU_{db} is the energy dissipated during bending of the peeling arm near the peel front.

The value of G_a is considered to be a "geometry-independent" parameter which characterises the fracture of the laminate. It reflects the energy to break the interfacial bonding forces and the energy dissipated *locally* ahead of the peel front in the plastic or viscoelastic zone at the crack tip. Now, consider a peeling arm of thickness, h, and width, b, which is peeling in a steady state under a constant load, P, at an applied peel angle of θ, as shown in Figure 1 Then:

$$dU_{\text{ext}} = Pda(1 + \varepsilon_a - \cos\theta)$$

$$d(U_s + U_{dt}) = bhda\int_0^{\varepsilon_a} \sigma \cdot d\varepsilon \tag{2}$$

where ε_a is the tensile strain in the peeling arm.

Therefore, if the peeling arm is considered to have an infinite tensile stiffness (*i.e.* $\varepsilon_a = 0$) and a zero bending stiffness, assumptions which are frequently made and which give a test which is equivalent to peeling away a material which behaves as a piece of "infinitely-rigid string", then we obtain the simple equation:

$$G_a^{\infty E} = \frac{P}{b}(1 - \cos\theta) \tag{3}$$

If any tensile (*i.e.* stretching) deformation of the peeling arm is taken into account, but the bending of the peeling arm is assumed to be only elastic, then we obtain the equation:

$$G_a^{eb} = \frac{P}{b}(1 + \varepsilon_a - \cos\theta) - h\int_0^{\varepsilon_a} \sigma \cdot d\varepsilon \tag{4}$$

It should also be noted that the maximum elastic energy (per unit width per unit length), G^e_{max}, which can be stored in the peeling arm for an elastic, non-work hardening, material is given by:

$$G^e_{\text{max}} = \frac{\sigma\varepsilon_y h}{2} = \frac{E\varepsilon_y^2 h}{2} \tag{5}$$

where ε_y is the yield strain and E is the Young's modulus of the peeling arm (see Fig. 2 with $\alpha = 0$).

2.2. Local Plastic Bending

Now, if plastic, or viscoelastic, bending of the peeling arm occurs near the crack front, then the determination of G_a needs to take such energy losses into account. Thus, the value of G_a is given by:

$$G_a = \frac{P}{b}(1 + \varepsilon_a - \cos\theta) - h\int_0^{\varepsilon_a} \sigma \cdot d\varepsilon - G_{db} \tag{6}$$

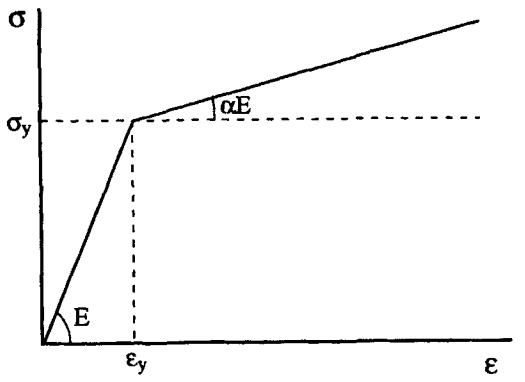

FIGURE 2 Bi-linear, work hardening stress *versus* strain curve.

where $G_{db} = dU_{db}/b \cdot da$. From Equation (4), an alternative representation of Equation (6) is, therefore:

$$G_a = G_a^{eb} - G_{db} \tag{7}$$

Obviously, the value of G_a^{eb} can be evaluated simply from Equation (4), and it is the evaluation of G_{db} which is needed to enable the determination of G_a.

2.3. Evaluation of G_{db}

The evaluation of G_{db} is complex. The first step has been modelling the peeling arm as a bilinear, work-hardening material, as shown in Figure 2. This form of model provides a good fit for the experimental stress *versus* strain curves for any polymers. Hence, the values of the modulus, E, plastic yield strain, ε_y, and the work-hardening parameter, α, can be ascertained. Next, using large displacement beam theory, the aspects of elastic-plastic loading, elastic-plastic unloading and root rotation at the peel front have all had to be considered[5-8]. This later consideration leads to the definition of the slope at the contact point, θ_o, see Figure 3. In Figure 3, the common

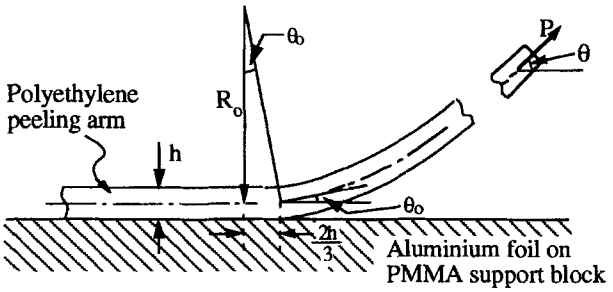

FIGURE 3 Root rotation in the peel test.

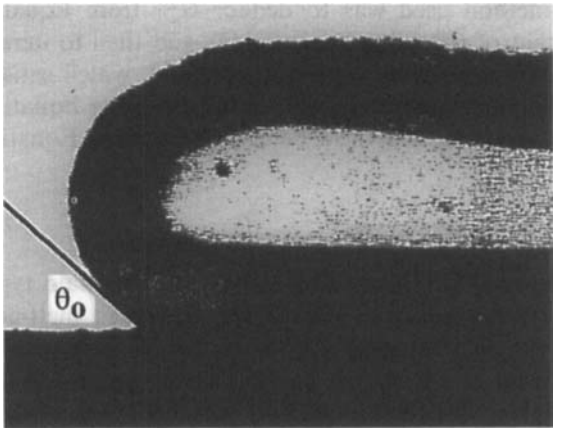

FIGURE 4 Optical micrograph of the peel front, PE1/A1-foil laminate; $\theta = 180°$; $h = 75$ μm; rate of test = 1 mm/min. (Peeling from left to right; taken at × 200 magnification.)

approach[9] of extending the length of the "beam" by $2h/3$ has been adopted to allow for the fact that the beam does *not* act as a truly built-in beam. An interesting secondary point, that arises from recognising that the slope at the peel front does not have to be zero, is the ability to partition the applied energy between that which is transmitted *via* bending of the arm, and the remaining portion which is transmitted directly to the peeling process. For example, if the value of $\theta_o = 0$, then the beam does act as a built-in beam and all the energy that is needed to fail the laminate has to be transmitted to the interfacial regions *via* bending of the polyethylene arm. If θ_o does not equal zero, then only a proportion of the energy to the peel front is delivered by bending, the rest going directly to the peeling process. (If the value of θ_o becomes equal to θ, then this means that the material has a zero bending modulus, and this is again equivalent to peeling away a material which behaves as "string", and all the energy for peeling is transmitted directly, *none* goes *via* bending of the arm.)

Now it can be shown[7,8] that:

$$\theta_o = \frac{4\varepsilon_y k_o}{3} \tag{8}$$

$$\frac{G_{db}}{G^e_{\max}} = f_1(k_o) \tag{9}$$

$$\frac{G_a^{\infty E}}{G^e_{\max}} \cdot \frac{1 - \cos(\theta - \theta_o)}{1 - \cos\theta} = f_2(k_o) \tag{10}$$

where the term, k_0, is given by R_1/R_o. Now R_o is the actual radius of curvature at the peeling front (see Fig. 3), R_1 is the radius of curvature at the onset of plastic yielding ($R_1 = h/2\varepsilon_y$), and $f_1(k_o)$ and $f_2(k_o)$ are functions (see the Appendix). To determine the

value of G_{db} the method used was to deduce $G_a^{\infty E}$ from Equation (3), $G^e_{\max}$ from Equation (5) and that of G_a^{eb} using Equation (4), and then to iterate between Equation (8) and (10) todetermine the values of k_0 and θ_0 which satisfied both of these equations. Next, the value of G_{db} may be determined using Equation (9). Finally, the adhesive fracture energy, G_a, may now be calculated using Equation (7).

3. MATERIAL AND TEST METHODS

Several different types of laminates were employed. The main types examined consisted of low-density polyethylene films which had been melt-adhered directly to aluminium foil. Two different grades of polyethylene were used which possessed different tensile stress *versus* strain curves. These are termed PE1/A1-foil and PE2/A1-foil laminates. The aluminium foil was firmly bonded to a flat support block of poly(methyl methacrylate) (PMMA) and the polymeric film was peeled away from the aluminium foil. A linear-bearing trolley was used to maintain a constant peel angle, θ, which was determined by the angle of the poly(methyl methacrylate) support block. This test arrangement is shown in Figure 1. Apart from recording the force, P, needed to peel away the polyethylene film from the aluminium foil, the strain in the arm of the film was also determined. In separate tests, the stress, σ, *versus* strain, ε, curve of the polyethylene films was determined from conducting uniaxial tensile tests using dumb bell-shaped specimens of the films. Finally, to examine the accuracy of the theory developed above, a mini peel-rig was built which enabled the peel test as shown in Figure 1 to be undertaken whilst still and video pictures were taken using an optical stereo microscope. Also examined was a poly(ethylene terephthalate) (PET) film which was adhered to polyethylene, the poly(ethylene terephthalate) film being peeled away from the polyethylene which was bonded firmly down to the PMMA support block.

4. RESULTS AND DISCUSSION

The results are shown in Tables I and II.

TABLE I

Results for PE2/A1-foil laminates

Peel angle (°)	$G_a^{\infty E}$(J/m^2)	θ_0(theory)(°)	θ_0(expt.)(°)	G_a(J/m^2)
45	183	20.4	24 to 30	236
90	333	34.5	40 to 47	228
120	375	41.7	48 to 58	218
135	412	46.1	50 to 60	223
150	467	51.7	55 to 62	236

Notes: $\varepsilon_y = 7.8\%$; $E = 140$ MPa; $\alpha = 0.1$; $h = 35$ μm. $G^e_{\max} = 15.9$ J/m^2 from Equation (5). $G_a^{\infty E}$ from Equation (3). θ_0 (theory) from Equation (8). G_a from Equation (6) [or (7)].

TABLE II
Results for the PET/PE laminates

Peel angle (°)	$G_a^{\infty E}$ (J/m^2)	θ_0(theory)(°)	θ_0(expt.)(°)	G_a(J/m^2)
30	44.2	5.3	5 to 10	24.6
60	80.0	8.0	8 to 12	29.7
90	78.0	8.5	8 to 13	22.8
120	90.0	9.6	9 to 14	21.3
150	119.0	11.8	10 to 15	22.0

Notes: $\varepsilon_y = 2.4\%$; E = 3800 MPa; $\alpha = 0.03$; h = 10 μm. $G^e_{max} = 11$ J/m^2 from Equation (5). $G_a^{\infty E}$ from Equation (3). θ_0 (theory) from Equation (8). G_a from Equation (6) [or (7)].

CONCLUSIONS

1. The value of $G_a^{\infty E}$ from Equation (3), which is the simplest way of deriving a value of the peeling energy for different values of peel angle, θ, is very dependent upon the peeling angle used. It does not provide a "material parameter" for characterising the peel test.
2. However, when corrections are made for the energy dissipated in the tensile stretching and bending of the peeling arm, the value of G_a may be derived from Equation (6) or (7), using the analysis outlined above. As may be seen, within experimental error, the value of G_a is independent of the peel angle. It is also found[8] to be independent of the thickness of the film which is being peeled away. Indeed, the above analysis explains many of the experimental observations previously reported in the literature. The value of G_a may, therefore, be used as a "material parameter" for characterising the peeling process.
3. The analysis is also confirmed by measuring the angle at the peel front, θ_0 (expt.), using a mini peel-rig mounted on the stage of a stereo opticl microscope. The experimental measurements are in excellent agreement with the theoretical values (*i.e.* θ_0 (theory)) from the above, analysis.

Acknowledgements

The authors would like to acknowledge the support of Tetra Pak, Romont, Switzerland and, in particular, the encouragement and help from Dr. Anne Roulin.

References

1. Y. Inoue and Y. Kobatake, *Applied Sci. Research*, **A8**, 321(1959).
2. T. Hata, M. Gamo and Y. Doi, *Kobienshi Kagaku*, **22**, 152(1965).
3. A. N. Gent and G. R. Hamed, *J. Applied Polymer Sci.*, **21**, 2817(1977).
4. A. J. Kinloch, *Adhesion and Adhesives: Science and Technology*, (Chapman Hall, London, 1987), p. 302.
5. K. S. Kim and J. Kim, *Trans. ASME*, **110**, 266(1988).
6. N. Aravas, K. S. Kim and M. J. Loukis, *Mater. Sci. Eng.*, **A107**, 159(1989).
7. J. G. Williams, *J. Adhesion*, **41**, 225(1993).
8. A. J. Kinloch, C. C. Lau and J. G. Williams, *Int. J. Fracture*, **66**, 45 (1994).
9. S. Hashemi, A. J. Kinloch and J. G. Williams, *Proc., Royal Soc.*, **A427**, 173(1990).

Appendix

For $\alpha < 0.5$ and $k_o > \dfrac{2(1-\alpha)}{(1-2\alpha)}$ then:

$$f_1(k_o) = \frac{4}{3}\alpha(1-\alpha)^2 k_o^2 + 2(1-\alpha)^2(1-2\alpha)k_o + \frac{2(1-\alpha)}{3(1-2\alpha)k_o}[1+4(1-\alpha)^3] - (1-\alpha)[1+4(1-\alpha)^2]$$

$$f_2(k_o) = \frac{\alpha}{3}[1+4(1-\alpha)^2]k_o^2 + 2(1-\alpha)^2(1-2\alpha)k_o + \frac{8}{3}\frac{(1-\alpha)^4}{(1-2\alpha)k_o} - 4(1-\alpha)^3$$